# STUDY ON THE DAMAGE PROPAGATION OF A COMPOSITE SANDWICH PANEL WITH FOAM CORE AFTER LOW VELOCITY IMPACT

Z.H. Xie*, J. Tian, J. Zhao, W. Li, T.J. Zhao, X. Li
College of Astronautics, Northwestern Polytechnical University, Xi'an, China
* Corresponding author(xzhae@nwpu.edu.cn)

**Keywords**: *sandwich structures, foam core, low-velocity impact damage, analytical model*

## 1 Introduction

Aerospace composite sandwich structures with two composite laminate facesheets bonded by a light-weight core material (honeycomb or foam core), can provide an excellent bending stiffness and a high specific strength and stiffness. These sandwich panels were more sensitive to a low-velocity impact damage than metal. Numerous studies reported that low-velocity impact or low-energy impact, such as tool-drop, runway stones, hailstone and tire blowout debris, may result in an indentation that undetectable or barely detectable by visual inspection, cause internal damage of the structures in form of matrix cracking, fiber damage, face sheet debonding and delamination, and core crushing [1-4], and can lead to a substantial decrease of load bearing capability of the structures [5].

One of the key issues associated with use of composite sandwich in aircraft structures was their damage resistance and damage tolerance [6,7]. Damage resistance of composite sandwich panel was concerned with the creation of damage due to a specific impact event. Here the characteristic index included the form of the damage, the range of the damage and the grade of the damage in a custom impact event. Damage tolerance of composite sandwich panel was concerned with the structural response and integrity associated with a given damage state of a structure. Here the characteristic index included the failure mode , damage propagation and residual strength of the composite sandwich panel with low-velocity impact in a custom loading mode. Damage tolerance for composite sandwich structures was typically determined based on test data and finite element method (FEM) [6]. For composite sandwich structures, post-impact compressive strength after impact using a Sandwich Compression After Impact (SCAI) test should be used to characterize the low impact damage tolerance of composite sandwich structures.

Composite sandwich structures bonded to foam core relative to bonded to honeycomb, had a bright future, owing to its smooth surface, low moisture absorption and easy molding. This paper introduces the work on the SCAI test on composite sandwich panels with foam core and an analytical model that can successfully predict the damage propagation behavior of a foam core sandwich panel with a low-velocity impact damage.

## 2 Experimentation

### 2.1 Global and Local Crushing Tests on Foam Cores

The global crushing tests on foam cores were designed and conducted by referencing the ASTM C365-5 test standard in order to determine the behaviour of the foam core. The dimensions of the test specimen which was made of 71WF-HT polymethacrylimide (PMI) foam were 50mm× 50mm×10mm. The apparatus of the flatwise compression test of the foam core was shown in Fig. 1. Apply a compressive force to the specimen at the rates of 0.5mm/min while recording data such as the displacement of the indenter and the load.

The flatwise core crushing tests revealed the nonlinear behavior of foam core under compression along the thickness direction as shown in Fig. 2. In this plot, the stress was defined as the compressive force divided by the cross sectional area of the core. The elastic region of the stress-strain curve was determined by the value of the Young's modulus $E_{zz}^{core}$. There exists an ultimate strength $(\sigma_3^{core})_{ultimate}$

corresponding to the core crippling. After the initiation of the core crushing, the stress nearly remained constant while the strain increasing resulting in a plateau section in the stress-strain curve.

The equivalent local core stiffness coefficient $k_{cf}^{eq}$ which was the function of the out-of-plane modulus $E_{zz}^{core}$ and two shear modulus $G_{xz}^{core}$ and $G_{yz}^{core}$ of the foam core can be obtained through the local core crushing test, as shown in Fig. 3, in which tups with different diameters were used. Linear regression was used to fit a line to the test data and the equivalent local stiffness $k_{cf}^{eq}$ was estimated as show in Fig. 4. According to experimental results for the foam core material, the equivalent local core stiffness coefficient $k_{cf}^{eq}$ was roughly two times of the out-of-plane stiffness $k_{zz}$ that was obtained from the flatwise normal core crushing.

**2.2 SCAI Test of Foam Core Sandwich Panels**

Sandwich Compression After Impact (SCAI) test on composite sandwich panels with foam core was conducted according to ASTM standard test method of ASTM D7137/D7137M-07. The dimensions of specimens were 150mm×100mm×13mm. The facesheets were made of T700/6421 laminates with the layup $[45/0/-45/90]_S$, and the core was 71WF-HT PMI foam with 10mm thickness. The mechanical properties of T700/6421 was given in Table 1. An impactor with 10 Joules impact energy was used to introduce the low-velocity impact damage on the sandwich specimens.

Displacement-controlled SCAI tests of composite sandwich panels were conducted in a universal testing machine operated at the load rate of 1.25 mm/min until the panels ruptured. A total of seven strain gages were used: five strain gages were positioned on the impacted face and two strain gages on the backside, as shown in Fig. 5. The two strain gages (gage#1 and gage#2) positioned on the impacted facesheet, along with backside strain gages (gage#3 and gage#4) were used to measure far-field strain and to control strain distribution which was useful in determining if the bending was being introduced between two facesheets. The strain gages gage#5, gage#6 and gage#7 were positioned along the line, which was vertical with the load direction, passed the center of the indentation of the impacted facesheet, and away from the center of the crushed core 10mm, 25mm and 35mm respectively.

The SCAI test fixture as designed in ASTM D7137/D7137M-07 was shown in Fig. 6. In this standard test fixture, the top and bottom supports provide no clamp-up, but provide some restraint to local out-of-plane rotation due to the fixture geometry. The side supports are knife edges, which provide no rotational restraint [8].

During the SCAI test, with the increasing of compressive load along the longitudinal direction, the impact damage propagated along the transverse direction and the impact side failed first due to the damage propagation and the facesheet on impacted side buckles right after it, as show in Fig. 7.

The curves of far field stress vs. strain gage read on different locations along the damage propagation path were plot in Fig. 8, where the far field stress was defined as the total compressive load divided by the sum of the cross sectional area of the two facesheets. Before the failure of the facesheet, far field stress vs. far field strain (in gage#1) was linear in shape. The far field stress corresponding to the local strain on the propagation path of the damage was contained linear section and nonlinear section. Although the transition of the linear section and nonlinear section was smooth because of the excellent ductility of the facesheets, it was clearly to see that the far field stress of the transition point was rising with the increasing of the distance between the strain gages and the center of the indentation. The transition points were corresponds to the damage propagation reached to the location of the strain gages respectively, and at those critical time the foam under the strain gages began crushing, which caused the leap of the local strain. When the damage propagated to a certain critical location, catastrophic failure will occur. The residual load capacity of a composite sandwich panel subjected to low velocity impact was equivalent to the applied far field stress level when damage propagation reached to the location near the damage region.

## 3 Numerical Study by Using an Analytical Model

Because of the thickness of the core was dozens times than facesheet in the typical aerospace composite sandwich structures, only the damaged facesheet was modeled in the analytical model by assuming the undamaged facesheet had a negligible influence on the damage propagation. The damaged facesheet was modeled as an angle-ply composite laminate, which had an initial deflection in shape and was partially supported by an elastic foundation. The initial indentation and initially crushed core were included in the model as the most important damage modes [9].

The equations of compatibility and equilibrium were derived as follows from the Classical Laminated Plate Theory (CLPT) and the Principle of Virtual Work.

Compatibility equation:

$$\begin{aligned} &t[A_{22}^{*}\psi_{,xxxx} - 2A_{26}^{*}\psi_{,xxxy} + (2A_{12}^{*} + A_{66}^{*})\psi_{,xxyy} - \\ &2A_{16}^{*}\psi_{,xyyy} + A_{11}^{*}\psi_{,yyyy}] - B_{21}^{*}w_{,xxxx} + \\ &(B_{62}^{*} - 2B_{16}^{*})w_{,xyyy} + (2B_{66}^{*} - B_{11}^{*} - B_{22}^{*})w_{,xxyy} + \\ &(B_{61}^{*} - 2B_{26}^{*})w_{,xxxy} - B_{12}^{*}w_{,yyyy} = w_{,xy}^{2} - \\ &w_{,xx}w_{,yy} - \xi_{,xx}w_{,yy} - \xi_{,yy}w_{,xx} + 2\xi_{,xy}w_{,xy} \end{aligned} \quad (1)$$

Equilibrium equation:

$$\begin{aligned} &t[B_{21}^{*}\psi_{,xxxx} + (2B_{26}^{*} - B_{61}^{*})\psi_{,xxxy} + (B_{11}^{*} + \\ &B_{22}^{*} - 2B_{66}^{*})\psi_{,xxyy} + (2B_{16}^{*} - B_{62}^{*})\psi_{,xyyy} + \\ &B_{12}^{*}\psi_{,yyyy}] + D_{11}^{*}w_{,xxxx} + 4D_{16}^{*}w_{,xxxy} + \\ &2(D_{12}^{*} + 2D_{66}^{*})w_{,xxyy} + 4D_{26}^{*}w_{,xyyy} + D_{22}^{*}w_{,yyyy} - \\ &t\psi_{,yy}(w_{,xx} + \xi_{,xx}) + 2t\psi_{,xy}(w_{,xy} + \xi_{,xy}) - \\ &t\psi_{,xx}(w_{,yy} + \xi_{,yy}) + q_{cf} = 0 \end{aligned} \quad (2)$$

Where the function $\xi(x, y)$ represented the residual deflection due to the impact and the function $q_{cf}(x, y)$ represented the elastic foundation of the core to the face sheet.

$$q_{cf} = q_{cf}^{e} + q_{cf}^{c} \quad (3)$$

Where $q_{cf}^{e}(x, y)$ represented the elastic part of the reaction stress for an undamaged core and $q_{cf}^{c}$ was the complementary item to incorporate the effect of core crushing.

$$q_{cf}^{e}(x, y) = k_{cf}^{eq}(E_{zz}^{core}, G_{xz}^{core}, G_{yz}^{core})w \quad (4)$$

$$q_{cf}^{c}(x, y) = \begin{cases} -k_{cf}^{eq}w & \textit{for the core crushed position} \\ 0 & \textit{for all else} \end{cases} \quad (5)$$

Equation (1) and equation (2) together consisted of the system of governing equations with two unknows $w(x, y)$ and $\psi(x, y)$.

According to St Venant's principle, the boundary conditions have negligible influence on the region far away from the boundaries. It was interesting to note that the damage propagation initiated around the damage zone. Experiments had revealed that if the section of the panel was chosen to be wide enough, in specific, if the distance between the panel edge to the center of the indentation was more than three times of the dimension of damage, the boundary conditions do not influence the damage propagation behavior. Thus, the panel section was assumed to be simply supported at all the four edges to simplify the solution.

For the sandwich panels in this study, the facesheets could be made by unbalanced and unsymmetric laminate that shows tension-shearing and tension-torsion coupling behaviors. Therefore, the out-of-plane deflection $w(x, y)$ could be unsymmetric even through the external loadings and all the boundary conditions are symmetric with respect to the central lines x=a/2 and y=b/2. As a result, the Fourier series should include all the possible odd and even index numbers for a general case.

Under the in-plane uniaxial compression loading conditions, the solutions of the governing equations (1) and (2) were assumed to be in a form of double Fourier series as follows.

$$\begin{cases} \psi(x,y) = \sum_{k=0}^{\infty}\sum_{l=0}^{\infty} \psi_{kl} \cos(\frac{k\pi x}{a})\cos(\frac{l\pi y}{b}) + \bar{\sigma}_{yy}\frac{x^2}{2} \\ w(x,y) = \sum_{m=1}^{\infty}\sum_{n=1}^{\infty} w_{mn} \sin(\frac{m\pi x}{a})\sin(\frac{n\pi y}{b}) \\ \xi(x,y) = \sum_{m=1}^{\infty}\sum_{n=1}^{\infty} \xi_{mn} \sin(\frac{m\pi x}{a})\sin(\frac{n\pi y}{b}) \end{cases} \quad (6)$$

with $m,n = 1,2,3...,and\ k,l = 0,1,2,3...$ $\bar{\sigma}_{yy}$ represents the externally applied far-field stress. The core/facesheet reaction stress $q_{cf}(x,y)$ was expanded also into a double Fourier series:

$$q_{cf}(x,y) = \sum_{m}\sum_{n} q_{mn} \sin(\frac{m\pi x}{a})\sin(\frac{n\pi y}{b}) \quad (7)$$

where $m,n = 1,2,3...$

Substituted equations (6) and (7) into the compatibility equation (1) and the equilibrium equations (2), and the governing equations in discrete form had been derived. Taking a finite number of modes in each of the series of $w$ and $\psi$, governing equations can be solved for $w_{rs}$ and $\psi_{rs}$ through numerical iteration. The controlling parameter was the far field stress $\bar{\sigma}_{yy}$, which started from 0 and increases with a load step $\Delta\bar{\sigma}_{yy}$ until the solution method fails to converge. Once the function of $w(x,y)$ and $\psi(x,y)$ have been solved, the corresponding values of the stresses, the strains, the membrane forces and the bending moments could all be derived.

A mechanism to simulate the consequential core crushing was incorporated into the model. After each successful converged load step, if $q_{cf}^{c}(x,y)$ exceeded the critical core crushing strength value $\sigma_{core}^{crushing}$, it is assumed that consequential core crushing occurs around that specific location at the current loading step. A new gap between the core and facesheet was assumed to emerge at that location and its corresponding core reaction stress was set to zero in the following analysis from that point on. This mechanism enabled the model to capture the initiation of further core crushing as well as the continuous propagation of the crushed core zone until the final failure of the structure.

## 4 Comparison of the Numerical and Experimental Results

The input parameters of the analytical model contain: the geometry of composite foam sandwich structures, the configuration of composite laminates, the depth and size of the indentation damage and the crushed core, the elastic parameters of the facesheet and foam core, etc.

The numerical results from the analytical model were compared with the experimental data as shown in Fig. 9. The stress of the transition point was 104MPa from the analytical model. Compared with 101MPa from the experimental data, the error was within 4%. Before the transition point, the curves of the numerical and the experimental data agreed well. The difference of the curves were began from the transition point, which was mainly caused by that the analytical model cannot exactly predict the real condition when large core crushed.

## 5 Conclusion

Experiments showed that the core crushing was the main failure mode of the composite foam core sandwich structures with low-velocity impacted damage subject to in-plane uniaxial compression. Once the damage caused by core crushing propagated to a certain critical location, subsequent catastrophic failure will occur. The residual load capacity of a low velocity impacted composite sandwich panel was equivalent to the applied far field stress level necessary to propagate the damage to a characteristic location near the damage region.

The analytical model with the input parameters which can be determined easily can predict the residual strength and the damage propagation of composite foam core sandwich structures subjected to low-velocity-impact effectively.

Table.1. The mechanical properties of facesheet.

| $E_L$ (GPa) | $E_T$ (GPa) | $G_{LT}$ (GPa) | $\nu_{LT}$ |
|---|---|---|---|
| 126 | 10 | 4.58 | 0.285 |

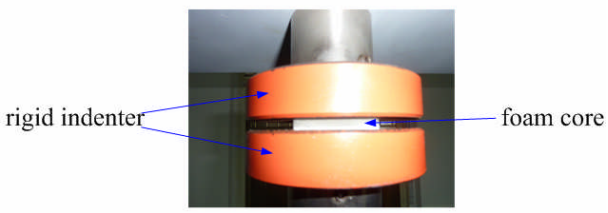


Fig. 1. The apparatus of the global core crushing test

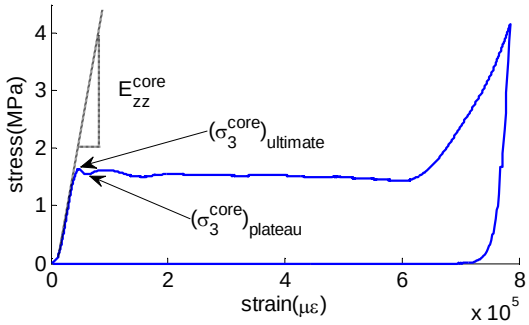


Fig. 2. Stress-strains curve for a flatwise compression test on foam core

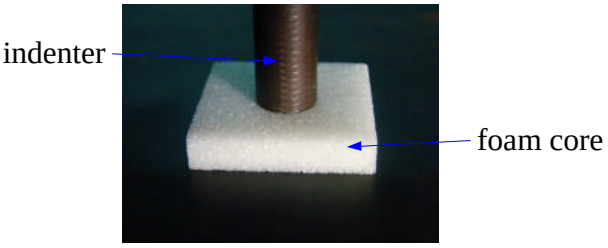


Fig. 3. The apparatus of the local core crushing test

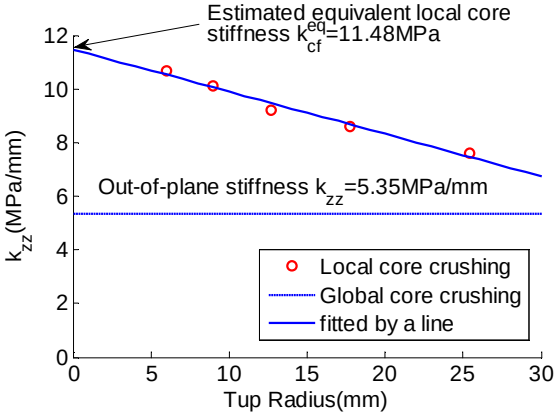


Fig. 4. Estimation of the equivalent local core stiffness

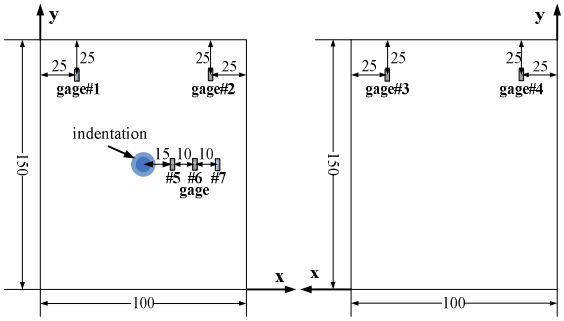


(a)The impacted face (b)The intact face

Fig. 5. A composite sandwich panel with strain gages (unit: mm)

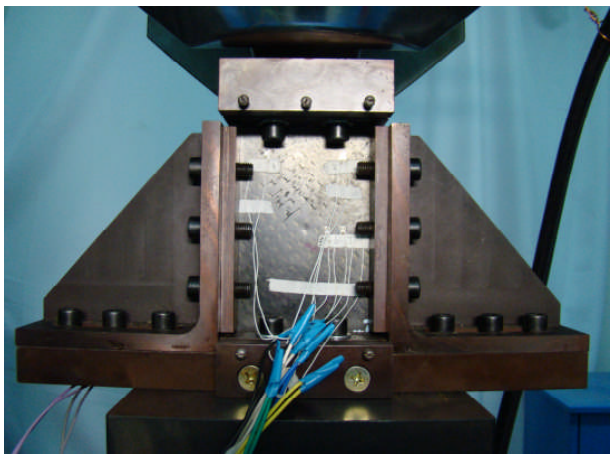

Fig. 6. The apparatus of the SCAI test with composite sandwich panel

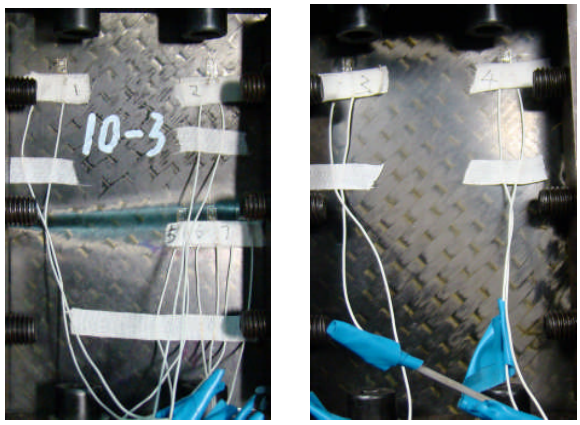


(a) Impacted side (b) Back side

Fig. 7. The form of damage in the SCAI test

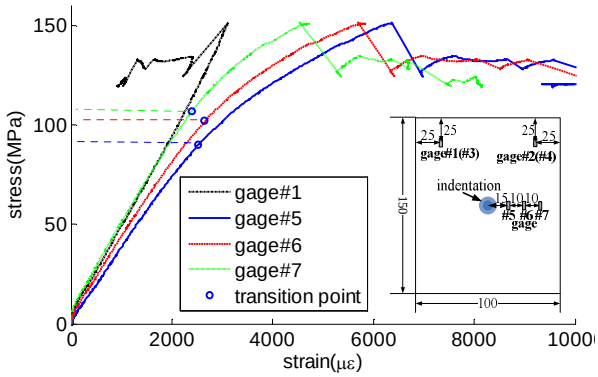


Fig. 8. Far field stress vs. strain: experimental

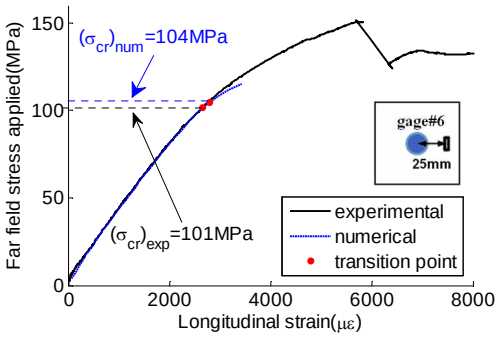


Fig. 9. Far field stress vs. local strain: experimental vs. numerical (at the location of gage #6)

## References


[1] Avery, W.B. and Grande, D.H., "Influence of Materials and Layup Parameters on Impact Damage Mechanisms," *Proceedings of the 22nd International Society for the Advancement of Materials and Process Engineering Technical Conference*, Vol.22, 1990, pp.470-483.

[2] Bull, P.H., "Damage Tolerance and Residual Strength of Composite Sandwich Structures," *Ph.D. Thesis, Department of Aeronautical and Vehicle Engineering, Kungliga Tekniska Hogskolan*, Stockholm, Sweden, 2004.

[3] Cantwell, W.J., Scudamore, R., Ratcliffe, J. and Davies, P., "Interfacial Fracture in Sandwich Laminates," *Composites Science and Technology*, Vol. 59, 1999, pp. 2079-2085.

[4] Nicholas, T.N., Zukas, J.A. and Swift, H.F., "*Impact Dynamics*," John Wiley & Sons, New York, 1982.

[5] Kassapoglou C, Jonas P J, Abbott R. "Compressive strength of composite sandwich panels after impact damage: an experimental and analytical study," *Journal of Composite Technology & Research*, 1988, 10: 65-73.

[6] Michael W. Czabaj, Alan T. Zehnder, Barry D. Davidson, Abhendra K. Singh, David P. Eisenberg. "Compression After Impact of Sandwich Composite Structures: Experiments and Modeling," *51st AIAA/ASME/ASCE/AHS/ASC Structures, Structural Dynamics, and Materials Conference*, April 12-15, 2010, Florida, AIAA 2010-2867, pp. 1-16.

[7] J. Tomblin, T. Lacy, B. Smith, S. Hooper, A. Vizzini, and S. Lee. "Review of Damage Tolerance for Composite Sandwich Airframe Structures," *Federal aviation administration report* No. DOT/FAA/AR-99/49, 1999.

[8] ASTM D7137/D7137M-07, "Standard Test Method for Compressive Residual Strength Properties of Damaged Polymer Matrix Composite Plates," *ASTM International*, 2007.

[9] Xie Zonghong, Vizzini A J. "Damage propagation in a composite sandwich panel subjected to increasing uniaxial compression after low-velocity impact," *Journal of Sandwich Structures and Materials*, 2005, 7:269-288.